J Fluoresc (2015) 25:441–449
DOI 10.1007/s10895-015-1531-3

ORIGINAL PAPER

Bi-8-carboxamidoquinoline Derivatives for the Fluorescent Recognition of Zn^{2+}

Xuhua Tian · Xiangfeng Guo · Lihua Jia · Yu Zhang

Received: 1 August 2014 / Accepted: 18 February 2015 / Published online: 27 February 2015

Abstract Three fluorescent sensors which were composed of a phendiol (*o*-, *m*-, *p*-isomers) and two carboxamidoquinolines have been synthesized and characterized. Research on the Zn^{2+}-sensing properties of the three sensors was carried out, and the results showed a significant difference in the recognition performance for Zn^{2+}. The fluorescence intensity ($I_{510\ nm}$) of ortho isomeric sensor binding to Zn^{2+} was enhanced 23-fold, the meta 15-fold, the para 8-fold. As the distance between two carboxamidoquinolines became longer, the fluorescence enhancement decreased. In addition, the selectivity of sensors got poor and the detection limit became higher with rising the distance between two receptors.

Keywords Carboxamidoquinolines · Fluorescent sensor · Zinc ion · Recognition · Isomeric

Introduction

As the second most abundant transition metal ion in the human body [1], zinc ion involves in multiple biological processes and has close relationship with many diseases [2, 3]. Based on the above facts, it is very necessary to monitor zinc ion. Fluorescence detection owing to their high sensitivity, selectivity, versatility and relatively simple handling has been widely implemented in biology and clinical medicine [4–7], especially for the detection of zinc ion.

The fluorescent sensors are the key to perform fluorescence detection. Thus, zinc ion fluorescent sensors have sparked the scientists' interest recently [8–10]. For satisfying the distinct demands, different kinds of fluorescent sensors for Zn^{2+} have been reported. So far, the reported Zn^{2+} sensors have commonly utilized courmarin [11, 12], naphthalimide [13], quinoline [14, 15], pyrene [16], anthracene [17, 18] etc. as fluorophores, and employed di-2-picolylamine [19], Schiff base [20, 21] and triazole [22, 23] etc. as the receptors. Among these, Zn^{2+} sensors based on carboxamidoquinoline developed quickly [24–26], owing to simple synthesis, certain binding ratio, good water-solubility, and ratio detection. In our previous research, the nitrogen atom at α position of the acetyl group was necessary to chelate Zn^{2+} [27]. Recently a combination of dual carboxamidoquinolines which have no the nitrogen atom at α position of the acetyl group could bind to Zn^{2+} successfully [28, 29].

It is generally known that the receptor with suitable distance of coordination atoms, matching shape and proper binding sites can improve the luminescent properties of a fluorescent sensor [30]. Herein, four fluorescent sensors (MQ, *o*-DQ, *m*-DQ and *p*-DQ) were synthesized through the introduction of carboxamidoquinoline on phenol and three isomers of phendiol (as shown in Scheme 1). The strategy is to modulate the distance and the number of coordination atoms by changing the number of carboxamidoquinolines and varying their substituent positions, and consequently the structure-function relationships of the sensors were discovered. The synthesis of the sensors followed the procedures in Scheme 1.

Electronic supplementary material The online version of this article (doi:10.1007/s10895-015-1531-3) contains supplementary material, which is available to authorized users.

X. Tian · X. Guo (✉) · L. Jia (✉) · Y. Zhang
College of Chemistry and Chemical Engineering, Key Laboratory of Fine Chemicals of College of Heilongjiang Province, Qiqihar University, Qiqihar 161006, China
e-mail: xfguo@163.com
e-mail: jlh29@163.com

Scheme 1 The synthesis of the sensors

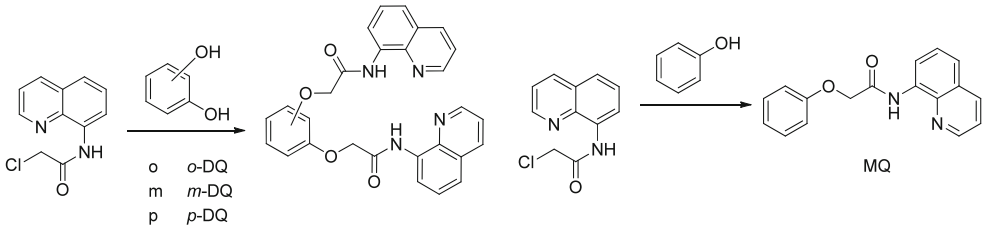

Experimental Section

Reagents and Apparatus

All solvents and reagents (analytical grade) were obtained commercially and used as received without further purification. Double-distilled water and HEPES buffer were used throughout the experiments. The metal ion solutions were prepared from NaCl, KCl, $Mg(ClO_4)_2$, $Ca(NO_3)_2$, $Cr(NO_3)_2$, $Fe_2(SO_4)_3$, $CoSO_4$, $NiSO_4$, $Cu(NO_3)_2$, $Zn(NO_3)_2$, $AgNO_3$, $CdSO_4$, $HgCl_2$, $Pb(NO_3)_2$, $AlCl_3$ in distilled water with a concentration of 0.05 M. All spectroscopic experiments were carried out at room temperature and pH is 8.3 in methanol/water (9:1, *v/v*) mixed solvent.

^1H NMR and ^{13}C NMR spectra were recorded on a Bruker AVANCE-600 spectrometer and referenced to internal tetramethylsilane. Infrared spectral data were measured with Nicolet Avatar-370. Mass spectra were obtained on a Waters Xevo G2-S QT. Melting points were measured using an X-6 microscopic melting point apparatus (Beijing, China). The UV–vis spectra were measured on a Puxi TU-1901 (Beijing, China) spectrophotometer. Fluorescence measurements were made on a Hitachi F-7000 (Tokyo, Japan). The excitation and emission slit widths were kept at 2.5 and 5.0 nm, respectively.

Preparation of 2-chloro-*N*-(quinol-8-yl)acetamide

2-Chloro-*N*-(quinol-8-yl)acetamide was synthesized by a modified procedure [31], 8-aminoquinoline 1.286 g (8.93 mmol) and potassium carbonate 3.703 g (26.79 mmol) were mixed in CH_2Cl_2 (25 mL), then the solution of the 2-chloroacetyl chloride 1.513 g (13.40 mmol) in dichloromethane (10 mL) was slowly added under cooling by ice. The resulting mixture was allowed to stir 2 h at room temperature. After filtration, the solvent was concentrated under vacuum. The crude products were purified by column chromatography using CH_2Cl_2 as eluant to afford a white solid. Yield: 1.691 g (85.9 %), mp: 132.1–132.6 °C.

Preparation of the Target Sensors

Phenol 0.051 g (0.53 mmol), potassium carbonate 0.147 g (1.06 mmol) and 2-chloro-*N*-(quinol-8-yl)acetamide 0.129 g (0.58 mmol) were mixed in anhydrous DMF (5 mL), the resulting mixture was kept stirring under N_2 atmosphere at 100 °C for 1 h. Then it was diluted by water and extracted with CH_2Cl_2. The organic layer was dried over magnesium sulfate and concentrated under reduced pressure. The crude

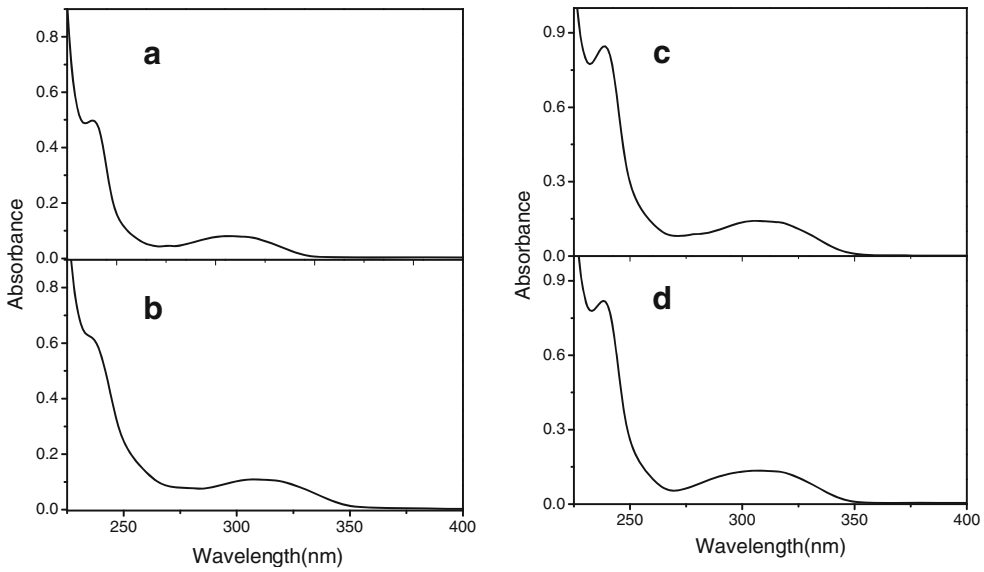

Fig. 1 Absorption spectra of sensors (10 μM). **a** MQ **b** *o*-DQ **c** *m*-DQ **d** *p*-DQ (methanol/water= 9:1, *v/v*, 0.01 M HEPES, pH=8.3)

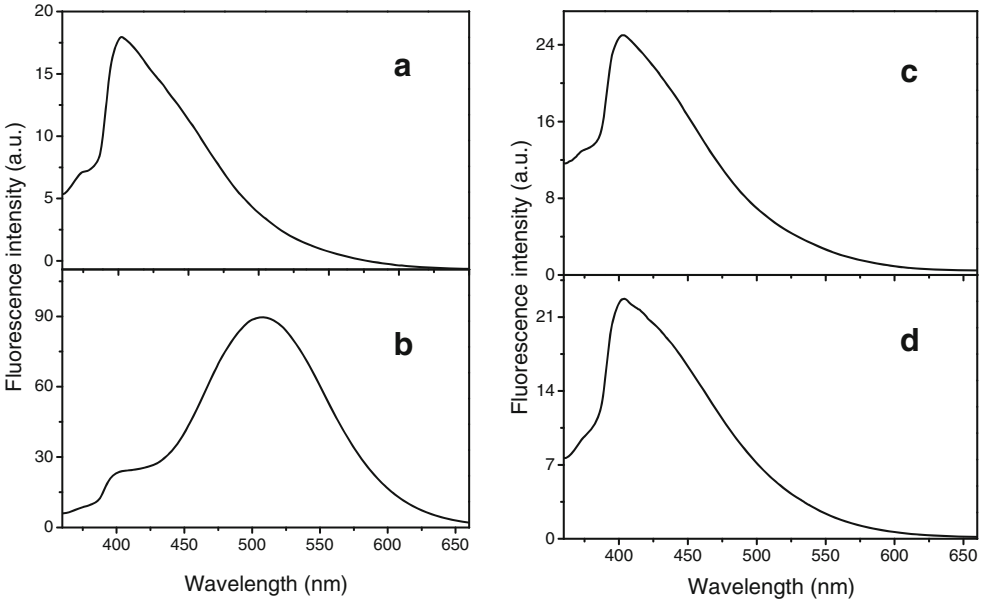

Fig. 2 Fluorescence spectra of sensors (10 μM). **a** MQ **b** *o*-DQ **c** *m*-DQ **d** *p*-DQ (methanol/water= 9:1, *v/v*, 0.01 M HEPES, pH=8.3, λ_{ex}=350 nm)

products were purified by column chromatography using CH_2Cl_2 as eluant.

Phendiol 0.045 g (0.41 mmol), potassium carbonate (4.0 eq.) and 2-chloro-*N*-(quinol-8-yl)acetamide (2.2 eq.) were mixed in anhydrous DMF (5 mL), the resulting mixture was kept stirring under N_2 atmosphere at 100 °C for 1 h. Then it was diluted by water and extracted with CH_2Cl_2. The organic layer was dried over magnesium sulfate and concentrated under reduced pressure. The crude products were purified by column chromatography using dichloromethane/ethyl acetate (20:1, *v/v*) as eluant.

Yields and spectral details of target sensors are given below.

MQ, 0.109 g, yield 72.7 %, mp: 107.5–108.6 °C. ^{1}H NMR (600 MHz, $CDCl_3$): δ 10.98 (s, 1H), 8.87 (dd, *J*=4.2, 1.7 Hz, 1H), 8.82 (dd, *J*=5.8, 3.1 Hz, 1H), 8.18 (dd, *J*=8.3, 1.7 Hz, 1H), 7.59-7.55 (m, 2H), 7.47 (dd, *J*=8.2, 4.2 Hz, 1H), 7.39-7.35 (m, 2H), 7.13 (dt, *J*=9.2, 1.7 Hz, 2H), 7.08-7.04 (m, 1H), 4.76 (s, 2H). ^{13}C NMR (150 MHz, $CDCl_3$): δ 166.80, 157.42, 148.61, 138.76, 136.19, 133.71, 129.75, 127.97, 127.21, 122.20, 122.19, 121.68, 116.79, 115.13, 68.14. FTIR(cm^{-1}): 3313, 3047, 2921, 1679, 1593, 1548, 1241, 1066. MS (ESI): *m/z* calcd for $C_{17}H_{15}N_2O_2^+$ ($M + H^+$) 279.1133, found 279.1301.

o-DQ, 0.130 g, yield 66.5 %, mp: 218.1–219.0 °C. ^{1}H NMR ($CDCl_3$, 600 MHz): δ 11.104 (s, 2H), 8.68 (d, *J*= 7.2 Hz, 2H), 8.51 (d, *J*=4.2 Hz, 2H), 7.82 (d, *J*=8.4 Hz,

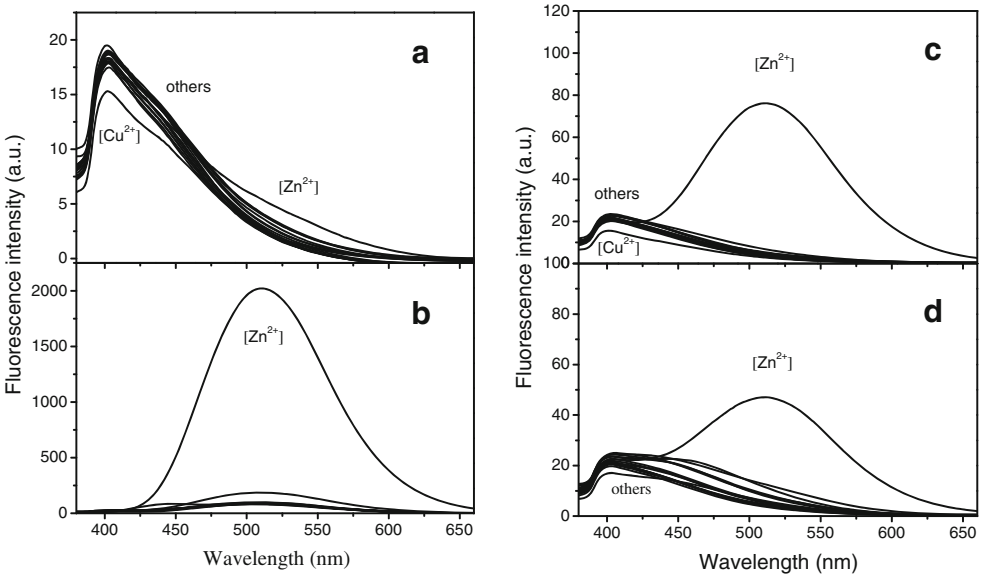

Fig. 3 Fluorescence spectra of sensors (10 μM) with different metal ions (10 μM) including Na^+, K^+, Mg^{2+}, Ca^{2+}, Cr^{3+}, Fe^{3+}, Co^{2+}, Ni^{2+}, Cu^{2+}, Zn^{2+}, Ag^+, Hg^{2+}, Cd^{2+}, Pb^{2+}, Al^{3+}. **a** MQ **b** *o*-DQ **c** *m*-DQ **d** *p*-DQ (methanol/ water=9:1, *v/v*, 0.01 M HEPES, pH=8.3, λ_{ex}=350 nm)

2H), 7.39 (t, *J*=7.8 Hz, 2H), 7.32 (d, *J*=8.4 Hz, 2H), 7.15-7.7.12 (m, 2H), 7.08-7.04 (m, 4H), 4.94 (s, 4H). ^{13}C NMR (150 MHz, $CDCl_3$): δ 166.66, 148.26, 147.68, 138.01, 135.43, 133.56, 127.34, 126.69, 122.91, 122.02, 121.32, 116.64, 114.82, 69.16. FTIR(cm^{-1}):3309, 3051, 2917, 1687, 1601, 1544, 1258, 1053. MS (ESI): *m/z* calcd for $C_{28}H_{23}N_4O_4^+$ ($M + H^+$) 479.1719, found 479.1873.

m-DQ, 0.133 g, yield 68.3 %, mp: 233.1–233.7 °C. ^{1}H NMR ($CDCl_3$, 600 MHz): δ 11.97 (s, 2H), 8.87 (dd, *J*= 1.8 Hz,1.8 Hz, 2H), 8.82 (q, *J*=3.0 Hz, 2H), 8.19 (dd, *J*= 0.6 Hz,1.2 Hz, 2H), 7.60-7.56 (m, 4H), 7.47 (q, *J*=4.2 Hz, 2H), 7.32 (t, *J*=8.4Hz, 1H), 6.97 (t, *J*=2.4 Hz, 1H), 6.80 (dd, *J*=2.4 Hz,2.4 Hz, 2H), 4.81 (s, 4H). ^{13}C NMR (150 MHz, $CDCl_3$): δ 166.49, 158.73, 148.64, 138.68, 136.25, 133.63, 130.59, 127.98, 127.21, 122.26, 121.71, 116.86, 108.64, 103.39, 68.99. FTIR(cm^{-1}):3321, 3047, 2908, 1691, 1610, 1548, 1184, 1066. MS (ESI): *m/z* calcd for $C_{28}H_{23}N_4O_4^+$ ($M + H^+$) 479.1719, found 479.1923.

p-DQ, 0.124 g, yield 63.7 %, mp: 231.4–232.4 °C. ^{1}H NMR ($CDCl_3$, 600 MHz): δ 10.95 (s, 2H), 8.85 (dd, *J*= 1.8 Hz,1.8 Hz, 2H), 8.82 (q, *J*=3.0 Hz, 2H), 8.18 (dd, *J*= 1.8 Hz,1.2 Hz, 2H), 7.58-7.56 (m, 4H), 7.47 (q, *J*=1.8 Hz, 2H), 7.13 (s, 4H), 4.81 (s, 4H). ^{13}C NMR (150 MHz, $CDCl_3$): δ 166.85, 152.75, 148.62, 138.75, 136.27, 133.70, 128.01, 127.25, 122.25, 121.71, 116.85, 116.49, 68.99. FTIR(cm^{-1}):3325, 3043, 2908, 1683, 1552, 1507, 1241, 1066. MS (ESI): *m/z* calcd for $C_{28}H_{23}N_4O_4^+$ ($M + H^+$) 479.1719, found 479.1941.

Results and Discussion

Absorption and Fluorescence Spectra of the Sensors

To investigate the effects of the number and position of substituents, UV and fluorescence spectra of four free sensors

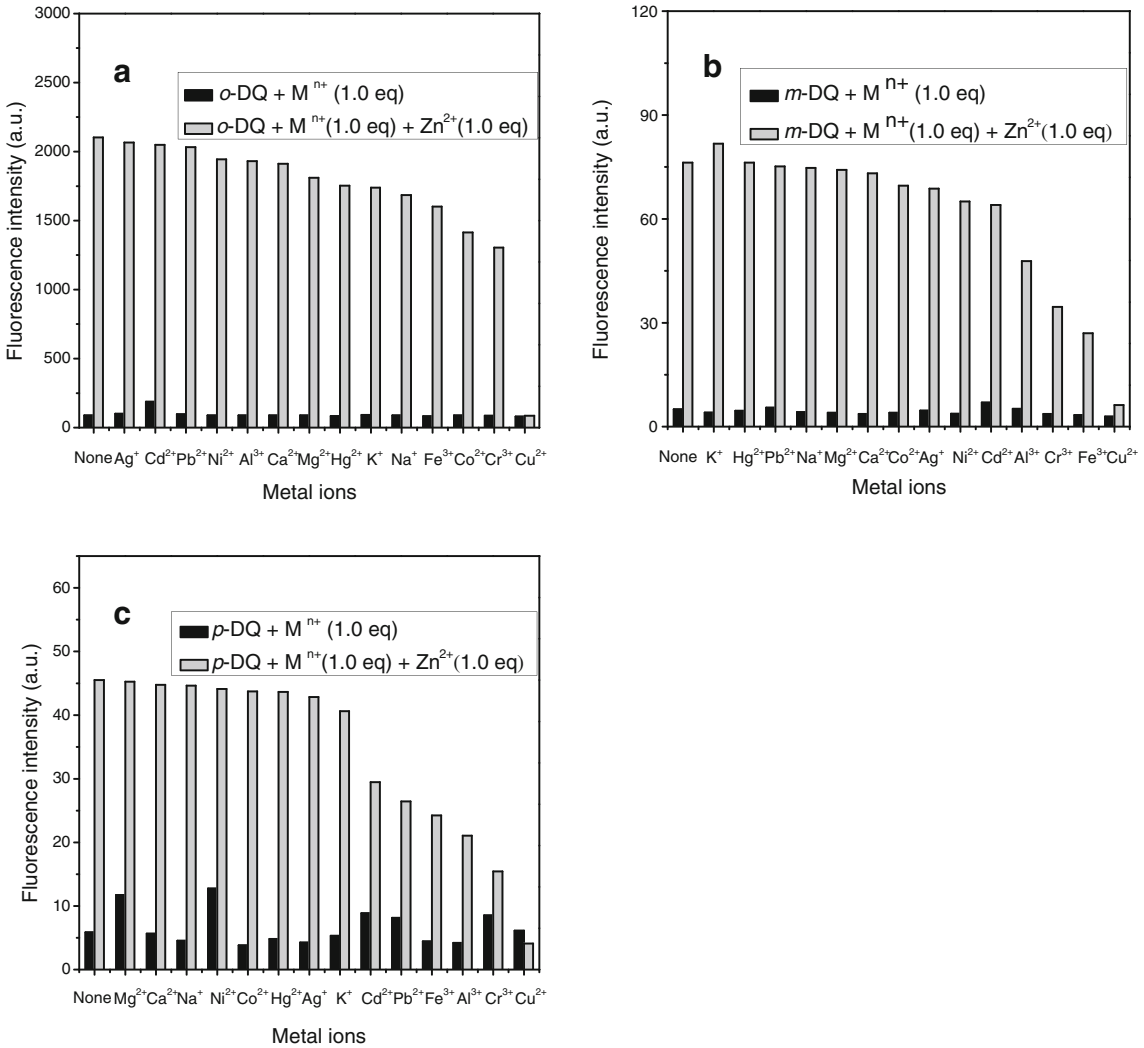

Fig. 4 Fluorescence response of sensors (10 μM) to various tested metal ions (10 μM) (black bar) and to the mixture of 10 μM of tested metal ions with 10 μM Zn^{2+} ion (*gray bar*). (λ_{ex}=350 nm, λ_{em}=510 nm) **a** *o*-DQ **b** *m*-DQ **c** *p*-DQ (methanol/water=9:1, *v/v*, pH=8.3, 0.01 M HEPES)

were obtained. As shown in Fig. 1, the maximum absorption wavelengths of the four compounds were at about 320 nm and the peak shapes were similar. All these suggested that the effects of the number and position of substituents on the conjugated system were not significant. That is to say, the ground electronic states of the four sensors had no obvious distinction.

It could be seen from Fig. 2, the three compounds (MQ, *m*-DQ, *p*-DQ) had similar peak shape and maximum emission wavelength around 400 nm, but the maximum emission wavelength of *o*-DQ shifted to 510 nm. The results showed that the excited electronic state of *o*-DQ was different from the others, which resulted from the effects of the number and position of substituents. The phenomenon may be explained as that a certain excited aggregation was formed because of the short distance of two carboxamidoquinoline groups of *o*-DQ, and the excited aggregation was easier to transfer the proton of the amide group to the nitrogen atom of quinoline, which broken the intermolecular hydrogen bonds and strengthened the ICT process [31, 32]. So the fluorescence spectrum of *o*-DQ was different from others.

Metal Ion Selectivity

Fluorescence spectra of four sensors were examined following the treatment with different metal ions (1.0 eq.) in methanol-water HEPES buffer solutions. As shown in Fig. 3, after adding Zn^{2+}, the fluorescence intensity ($I_{510\ nm}$) of *o*-DQ increased 23 times, while that of *m*-DQ and *p*-DQ increased 15 times and 8 times, respectively. The weaker binding capacity with a longer distance of two receptors caused that the fluorescence intensity of the compound became gradually weaker.

As may be seen in Fig. 3, the sensor of monocarboxamidoquinoline did not recognize Zn^{2+}, but the sensors of bicarboxamidoquinoline might identify Zn^{2+} via fluorescence enhancement with a red-shift. This indicated that the chelation process of Zn^{2+} binding was accomplished by the cooperation of two quinolyl groups. The bicarboxamidoquinoline ligand binding to Zn^{2+} raised the rigidity of the original fluorophore and induced chelation-enhanced fluorescence (CHEF) [33–35]. The deprotonation of amide NH by the induction of Zn^{2+} promoted the ICT process, which resulted in a 110 nm red-shift [36].

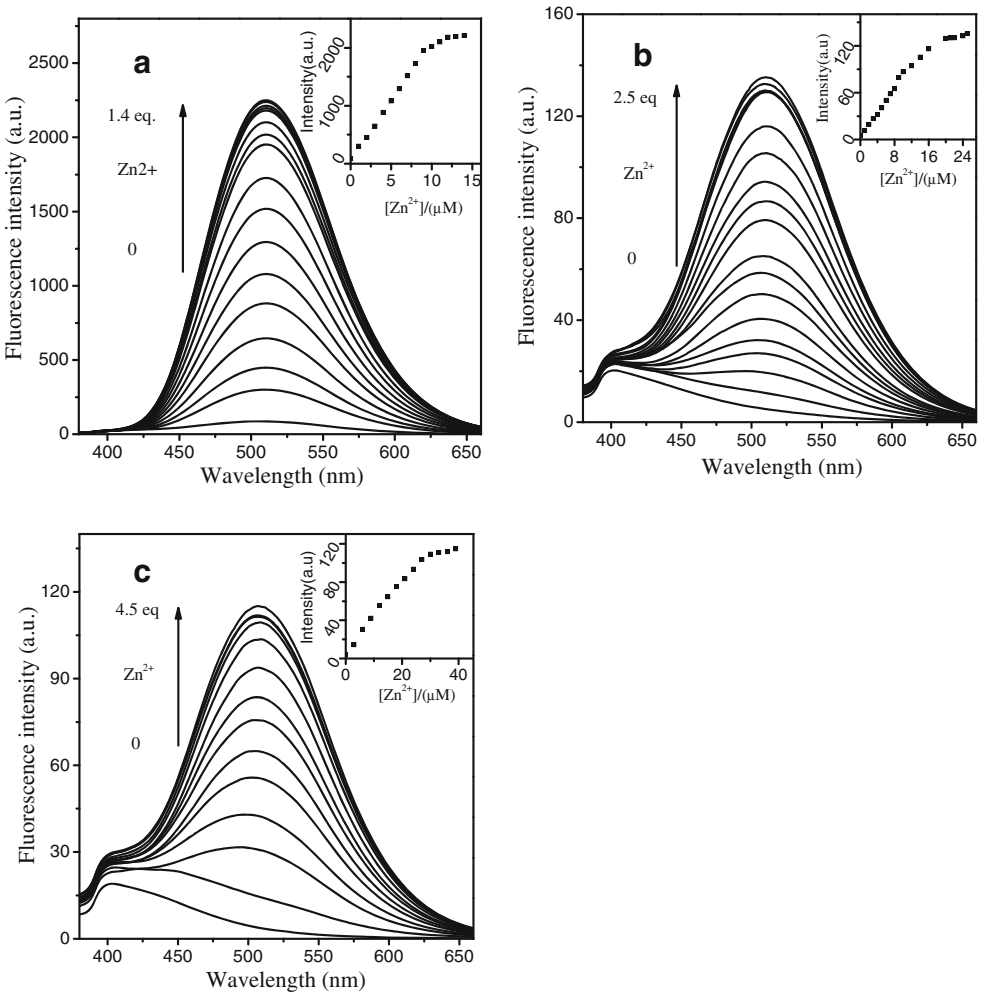

Fig. 5 Fluorescent spectra of sensors (10 μM) upon the addition of Zn^{2+}. Insert: Fluorescence intensity [I_{510nm}] as a function of Zn^{2+}concentration. **a** *o*-DQ **b** *m*-DQ **c** *p*-DQ (λ_{ex}= 350 nm, methanol/water=9:1, *v/v*, pH=8.3, 0.01 M HEPES)

Metal Ion Competition

In order to further test the interference of other common cations on the determination of Zn^{2+}, a competition experiment was carried out. As shown in Fig. 4, with the growing distance of two receptors, the number of metal ions species which could cause fluorescence quenching of sensor / Zn^{2+} complex increased gradually. A possible reason was that the sensor with a longer distance of receptors had a weaker binding capacity and was easily disturbed by other metal ions in recognition process, which was consistent with the reason of the decreasing intensity in Fig. 3.

Bonding Strength and Binding Model

The emission spectra of sensors were examined by fluorescence titrations. As shown in Fig. 5, the saturation emission at 510 nm decreased upon increasing distance of two receptors. This might be due to the decreasing binding capacity resulting from the increasing distance. As seen in the insert picture of Fig. 5, the maximum fluorescence intensity of *o*-DQ with 1.2 equiv. of Zn^{2+} was retained, the maximum fluorescence intensity of *m*-DQ with 2.0 equiv. of Zn^{2+} was retained, the maximum fluorescence intensity of *p*-DQ with 3.0 equiv. of Zn^{2+} was retained. The increasing changes in saturated complexation of the sensors revealed that the binding capacity decreased with increasing distance of two receptors, which confirmed the supposal of binding capacity above.

To study the binding capacity of the sensors, the binding constants of sensors with Zn^{2+} were determined from fluorescence titration data. As shown in Fig. 6, the binding constants which were obtained using the Benesi–Hildebrand equation [37, 38] were 2.21×10^4, 2.94×10^3 and 1.19×10^3 M^{-1} for *o*-DQ, *m*-DQ and *p*-DQ, respectively, which further confirmed the binding capacity decreased with the growing distance of receptors. Those are consistent with the conclusion from the insert picture of Fig. 5.

Based on the results and the 1:1 stoichiometry between sensors and Zn^{2+} derived from the job's plot curves (seen in

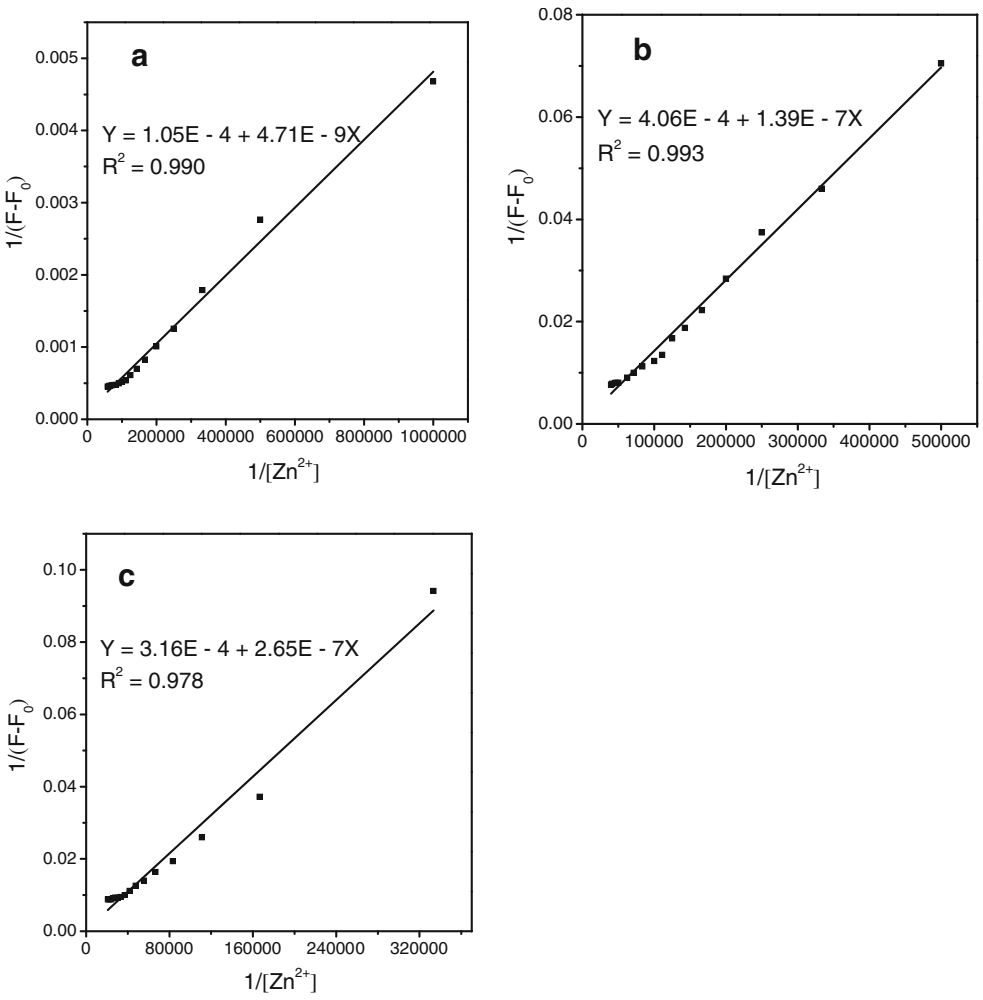

Fig. 6 Benesi–Hildebrand plot from fluorescence titration data of sensors (10 μM). **a** *o*-DQ **b** *m*-DQ **c** *p*-DQ (λ_{ex}=350 nm, λ_{em}= 510 nm, methanol/water=9:1, *v*/*v*, pH=8.3, 0.01 M HEPES)

Scheme 2 Probable binding model of sensors with Zn^{2+}

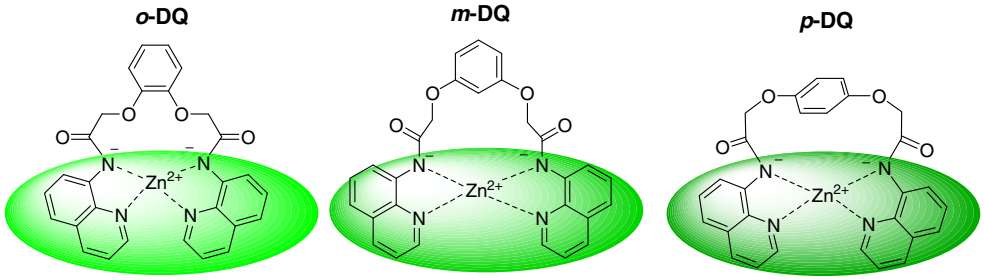

Fig. S1, supplementary material), the plausible binding model was proposed as Scheme 2.

Detection Limit

To study the variation regularity of the sensitivity of sensors, the detection limit of the sensors were obtained from Fig. 7. The determine limit of the *o*-DQ was 5.3×10^{-9} M, the *p*-DQ was 5.6×10^{-8} M, the *m*-DQ was 3.1×10^{-7} M. The increasing determine limit with the growing distance of receptors indicated the sensitivity became poor.

Conclusions

In summary, three sensors based on bicarboxamidoquinoline have been developed which can recognize Zn^{2+} with the different recognition performance. The fluorescent signal strength, the selectivity and sensitivity have been successfully

Fig. 7 Curve of fluorescence intensity at 510 nm of sensors versus increasing concentrations of Zn^{2+}. **a** *o*-DQ **b** *m*-DQ **c** *p*-DQ (λ_{ex}=350 nm, methanol/water= 9:1, *v*/*v*, pH=8.3, 0.01 M HEPES)

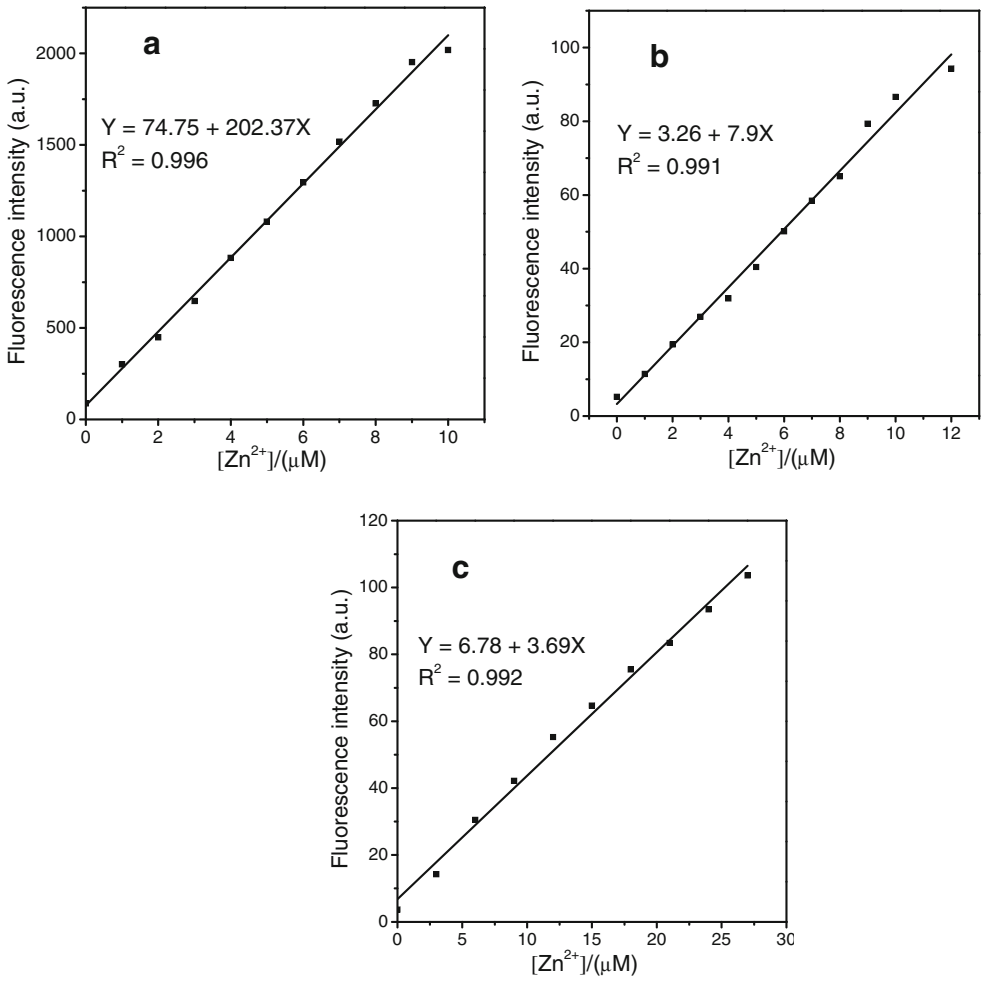

tuned by varying the substituent positions of bicarboxamidoquinoline. As the distance of receptors grew, the fluorescent intensity and the binding constant decreased, and the detection limit increased.

Acknowledgments This work was supported by the National Natural Science Foundation of China (21176125), the Science Research Project of the Ministry of Education of Heilongjiang Province of China (12521594, 2012TD012, JX201205), the Natural Science Foundation of Heilongjiang province of China (B201114, B201313), and the Key Program of Science and Technology of Qiqihar, Heilongjiang Province (GYGG–201108).

References

1. Andreini C, Banci L, Bertini I, Rosato A (2006) Zinc through the three domains of life. J Proteome Res 5:3173–3178
2. Frassinetti S, Bronzetti G, Caltavuturo L, Cini M, Croce CD (2006) The role of zinc in life: a review. J Environ Pathol Toxicol Oncol 25: 597–610
3. Cuajungco MP, Lees GJ (1997) Zinc metabolism in the brain: relevance to human neurodegenerative disorders. Neurobiol Dis 4:137–169
4. Wong LS, Khan F, Micklefield J (2009) Selective covalent protein immobilization: strategies and applications. Chem Rev 109:4025–4053
5. Yang Y, Zhao Q, Feng W, Li F (2013) Luminescent chemodosimeters for bioimaging. Chem Rev 113:192–270
6. Kobayashi H, Ogawa M, Alford R, Choyke PL, Urano Y (2010) New strategies for fluorescent probe design in medical diagnostic imaging. Chem Rev 110:2620–2640
7. Tomat E, Lippard SJ (2010) Imaging mobile zinc in biology. Curr Opin Chem Biol 14:225–230
8. Li X, Gao X, Shi W, Ma H (2014) Design strategies for water-soluble small molecular chromogenic and fluorogenic probes. Chem Rev 114:590–659
9. Xu ZC, Yoon JY, Spring DR (2010) Fluorescent chemosensors for Zn^{2+}. Chem Soc Rev 39:1996–2006
10. Carter KP, Young AM, Palmer AE (2014) Fluorescent sensors for measuring metal ions in living systems. Chem Rev 114:4564–4601
11. Simmons JT, Allen JR, Morris DR, Clark RJ, Levenson CW, Davidson MW, Zhu L (2013) Integrated and passive 1, 2, 3-triazolyl groups in fluorescent indicators for Zinc (II) ions: thermodynamic and kinetic evaluations. Inorg Chem 52:5838–5850
12. Sumiya S, Shiraishi Y, Hirai T (2013) Mechanism for different fluorescence response of a coumarin–amide–dipicolylamine linkage to Zn (II) and Cd (II) in water. J Phys Chem A 117:1474–1482
13. Zhang JF, Kim S, Han JH, Lee SJ, Pradhan T, Cao QY, Lee SJ, Kang C, Kim JS (2011) Pyrophosphate-selective fluorescent chemosensor based on 1, 8-naphthalimide–DPA–Zn (II) complex and its application for cell imaging. Org Lett 13:5294–5297
14. Meeusen JW, Tomasiewicz H, Nowakowski A, Petering DH (2011) TSQ (6-methoxy- 8-p-toluenesulfonamido-quinoline), a common fluorescent sensor for cellular zinc, images zinc proteins. Inorg Chem 50:7563–7573
15. Ravikumar I, Ghosh P (2011) Zinc (II) and PPi selective fluorescence OFF–ON–OFF functionality of a chemosensor in physiological conditions. Inorg Chem 50:4229–4231
16. Fernández-Lodeiro J, Núñez C, de Castro CS, Bértolo E, Seixas de Melo JS, Capelo JL, Lodeiro C (2013) Steady-state and time-resolved investigations on pyrene-based chemosensors. Inorg Chem 52:121–129
17. Basa PN, Bhowmick A, Horn LM, Sykes AG (2012) Zinc (II) mediated imine–enamine tautomerization. Org Lett 14:2698–2701
18. Ingale SA, Seela F (2012) A ratiometric fluorescent on–off Zn^{2+} chemosensor based on a tripropargylamine pyrene azide click adduct. J Org Chem 77:9352–9356
19. Lin W, Buccella D, Lippard SJ (2013) Visualization of peroxynitrite-induced changes of labile Zn^{2+} in the endoplasmic reticulum with benzoresorufin-based fluorescent probes. J Am Chem Soc 135: 13512–13520
20. Zhou Y, Li ZX, Zang SQ, Zhu YY, Zhang HY, Hou HW, Mak TCW (2012) A novel sensitive turn-on fluorescent Zn^{2+} chemosensor based on an easy to prepare C_3-symmetric schiff-base derivative in 100% aqueous solution. Org Lett 14:1214–1217
21. Wang L, Qin W, Tang X, Dou W, Liu W (2011) Development and applications of fluorescent indicators for Mg^{2+} and Zn^{2+}. J Phys Chem A 115:1609–1616
22. Pathak RK, Hinge VK, Mondal M, Rao CP (2011) Triazole-linked-thiophene conjugate of calix [4] arene: its selective recognition of Zn^{2+} and as biomimetic model in supporting the events of the metal detoxification and oxidative stress involving metallothionein. J Org Chem 76:10039–10049
23. Pathak RK, Tabbasum K, Rai A, Panda D, Rao CP (2012) Pyrophosphate sensing by a fluorescent Zn^{2+} bound triazole linked imino-thiophenyl conjugate of calix [4] arene in HEPES buffer medium: spectroscopy, microscopy, and cellular studies. Anal Chem 84: 5117–5123
24. Song EJ, Kang J, You GR, Park GJ, Kim Y, Kim SJ, Kim C, Harrison RG (2013) A single molecule that acts as a fluorescence sensor for zinc and cadmium and a colorimetric sensor for cobalt. Dalton Trans 42:15514–15520
25. Pal P, Rastogi SK, Gibson CM, Aston DE, Branen AL, Bitterwolf TE (2011) Fluorescence sensing of zinc (II) using ordered mesoporous silica material (MCM-41) functionalized with *N*-(quinolin-8-yl)-2-[3-(triethoxysilyl) propylamino] acetamide. ACS Appl Mater Interfaces 3:279–286
26. Rastogi SK, Pal P, Aston DE, Bitterwolf TE, Branen AL (2011) 8-Aminoquinoline functionalized silica nanoparticles: a fluorescent nanosensor for detection of divalent zinc in aqueous and in yeast cell suspension. ACS Appl Mater Interfaces 3:1731–1739
27. Zhang Y, Guo XF, Jia LH, Xu SC, Xu ZH, Zheng LB, Qian XH (2012) Substituent-dependent fluorescent sensors for zinc ions based on carboxamidoquinoline. Dalton Trans 41:11776–11782
28. Mummidivarapu VSS, Tabbasum K, Chinta JP, Rao CP (2012) 1, 3-Di-amidoquinoline conjugate of calix [4] arene (L) as a ratiometric and colorimetric sensor for Zn^{2+}: Spectroscopy, microscopy and computational studies. Dalton Trans 41:1671–1674
29. Tang LJ, Zhao J, Cai MJ, Zhou P, Zhong KL, Hou SH, Bian YJ (2013) An efficient sensor for relay recognition of Zn^{2+} and Cu^{2+} through fluorescence 'off–on–off' functionality. Tetrahedron Lett 54:6105–6109
30. Callan JF, de Silva AP, Magri DC (2005) Luminescent sensors and switches in the early 21st century. Tetrahedron 61:8551–8588
31. Zhang Y, Guo XF, Si WX, Jia LH, Qian XH (2008) Ratiometric and water-soluble fluorescent zinc sensor of carboxamidoquinoline with an alkoxyethylamino chain as receptor. Org Lett 10:473–476
32. Du JJ, Fan JL, Peng XJ, Li HL, Sun SG (2010) The quinoline derivative of ratiometric and sensitive fluorescent zinc probe based on deprotonation. Sensors Actuators B 144:337–341
33. Goswami S, Das AK, Aich K, Manna A, Maity S, Khanra K, Bhattacharyya N (2013) Ratiometric and absolute water-soluble fluorescent tripodal zinc sensor and its application in killing human lung cancer cells. Analyst 138:4593–4598
34. Yu H, Yu T, Sun M, Sun J, Zhang S, Wang S, Jiang H (2014) A symmetric pseudo salen based turn-on fluorescent probe for sensitive detection and visual analysis of zinc ion. Talanta 125:301–305

35. Lin HY, Cheng PY, Wan CF, Wu AT (2012) A turn-on and reversible fluorescence sensor for zinc ion. Analyst 137:4415–4417
36. Dong ZP, Guo YP, Tian X, Ma JT (2013) Quinoline group based fluorescent sensor for detecting zinc ions in aqueous media and its logic gate behaviour. J Lumin 134:635–639
37. Lee J, Kim H, Kim S, Noh JY, Song EJ, Kim C, Kim J (2013) Fluorescent dye containing phenol-pyridyl for selective detection of aluminum ions. Dyes Pigments 96:590–594
38. Goswami S, Maity S, Das AK, Maity AC (2013) Single chemosensor for highly selective colorimetric and fluorometric dual sensing of Cu (II) as well as 'NIRF' to acetate ion. Tetrahedron Lett 54:6631–6634